From colloids to nanotechnology: Investigations on magic nuclearity palladium nanocrystals

P. John Thomas and G. U. Kulkarni*

Nanolaboratory, Chemistry and Physics of Materials Unit, Jawaharlal Nehru Centre for Advanced Scientific Research, Jakkur, Bangalore 560 064, India

Current status of nanoscience research is briefly surveyed with special emphasis on monodisperse metal nanocrystals. Tunneling spectroscopy measurements on polymer protected magic nuclearity Pd_{561} nanocrystals have revealed single electron charging effects. Mesoscopic organizations resulting from self-assembly of these nanocrystals have been investigated. Giant clusters containing magic numbers of nanocrystals are formed when the nanocrystals are capped uniformly with a polymer. In contrast, alkanethiol capped nanocrystals yield well ordered two-dimensional arrays. The Pd nanocrystals have also been exploited as seeds to grow Ni overlayers of desired thickness to form Pd–Ni core-shell nanoparticles. Magnetic arrays of Pd–Ni nanoparticles have been obtained.

TWO centuries ago, the study of nanoscale solid particles, dispersed within a liquid host, played a pivotal role in establishing colloid science. Until the end of the last century, colloid science was, perhaps, something of an intellectual backwater – with few notable exceptions. However, significant advances in both experimental and theoretical aspects of the subject that took place during the last decade, and of course, the emergence of, and explosion of interest in the broad area of nanoscience and nanotechnology, have now set the scene for a renaissance in colloid science. Surprisingly, many workers in the modern field of nanoscience do not even recognize its colloidal source!

An important example of the parentage of the modern subject of metal nanoparticles derives from the work of Michel Faraday in the 1850's[1]. During those years, Faraday carried out groundbreaking studies of nanoscale gold particles in aqueous solution. He established the first scientific basis for the area, noting that the colloidal metal sols or pseudosolutions as he termed them, are thermodynamically unstable, and that the individual gold nanoparticles must be stabilized kinetically against aggregation. Once the nanoparticles coagulate, the process cannot be reversed. Remarkably, Faraday identified the very essence of the nature of colloidal, nanoscale particles of metals and specifically for the case of gold, he concluded '...the gold is reduced in exceedingly fine particles which becoming diffused, produce a beautiful fluid... the various preparations of gold whether ruby, green, violet or blue... consist of that substance in a metallic divided state'. Much later in 1905, Albert Einstein provided a thoroughly quantitative description for the state of colloidal dispersion on the basis of Brownian motion of the constituent particles[2].

Nanocrystals cover a size range 1–100 nm and are intermediate to the molecular size regime on one hand and the macroscopic bulk on the other. Chemically synthesized nanocrystals are kinetically stabilized against aggregation by a ligand shell present at the surface of the particle[3]. Conventional chemical synthesis of nanocrystals such as the method used by Faraday yields nanoparticles with ionic species at the surface of the nanoparticles and with a fairly wide distribution in diameter. Due to the ionic nature of the capping agents, the nanoparticle dispersions aggregate irreversibly upon solvent removal. These have been the major handicaps in the study of properties of nanocrystals and have led to an exploration of a host of synthetic strategies to stabilize nanocrystals by covalent ligands and thereby make them dispersible in a variety of solvents. Alkylamines, alkanethiols and phospholipids have been used as capping agents to prepare noble metal sols, dispersible reversibly in solvents such as toluene and chloroform[4]. Of late, newer synthetic strategies and post-preparation processing techniques like size-selective precipitation, have enabled excellent size control – to within 10% of the mean diameter. In this context, the synthesis of magic nuclearity nanocrystals assumes significance[4,5]. The magic numbers correspond to atoms filling up the coordination shells completely around a central atom in a close packed arrangement. Thus, the nuclearities 13, 55, 309, 561 and 1415, correspond to closure of one, two, four, five and seven shells respectively. The magic nuclearity nanocrystals are schematically illustrated in Figure 1. Cluster beam studies have identified that clusters or nanocrystals with a magic number of atoms tend to be more stable than other clusters of similar nuclearity[6]. Synthetic strategies have been formulated to obtain monodisperse nanocrystals such as Au_{55}, Pt_{309} and Pd_{561}. The preparation of magic nuclearity nanocrystals usually involves carefully controlled reducing conditions. Triphenylphosphine stabilized Au_{55} clusters have been made by reducing $AuPPh_3Cl$ with diborane[7] and Pd_{561} nanocrystals capped with phenanthroline have been made by hydrogen reduction of palladium acetate[8]. By varying

*For correspondence. (e-mail: kulkarni@jncasr.ac.in)

the concentration of the ethanolic solution of H_2PdCl_4, Teranishi and Miyake[9] have obtained a variety of polyvinylpyrolidone (PVP) capped Pd nanoparticles including Pd_{561}. The magic nuclearity nanocrystals so obtained are monodisperse (diameter distribution of $<4\%$). A scanning tunneling microscopy (STM) image as well as transmission electron micrograph (TEM) of the Pd_{561}–PVP nanocrystals are shown in Figure 2.

Another fascinating aspect of this field of research is related to the ability of the nanoparticles to spontaneously assemble into extended lattices[4]. Such mesoscopic assemblies are brought about by dispersion, steric and capillary forces, and are influenced by factors such as the capping agent employed and the size distribution of the nanocrystals. Nanocrystalline assemblies in the forms of strings as well as two-dimensional arrays of a variety of nanocrystals (Au, Ag, Pt, Pd, Co) have been obtained[4]. The assemblies lend themselves to unprecedented control, with both the interparticle spacing and the diameter of the nanocrystal being continuously variable. This has led to a renewed interest in the bottom-up approach to functional materials. Indeed, several applications have been envisaged for the nanocrystalline mesostructures, as for example, two-dimensional arrays of magnetic nanocrystals have been visualized as magnetic storage media[10]. Ensembles of nanoscopic objects such as nanotubes, nanowires and nanoparticles are considered important in the next generation electronic circuits[11].

Today, the overwhelming importance attached to the synthesis and manipulation of nanoscale objects means that the scene is once again set for this key subject to impact upon the development of not only chemistry, but also physics and materials science. In the following sections, we highlight a few of the key issues relating to metal nanocrystals where size determines their properties. Many of the experimental illustrations pertain to the magic nuclearity Pd_{561} cluster.

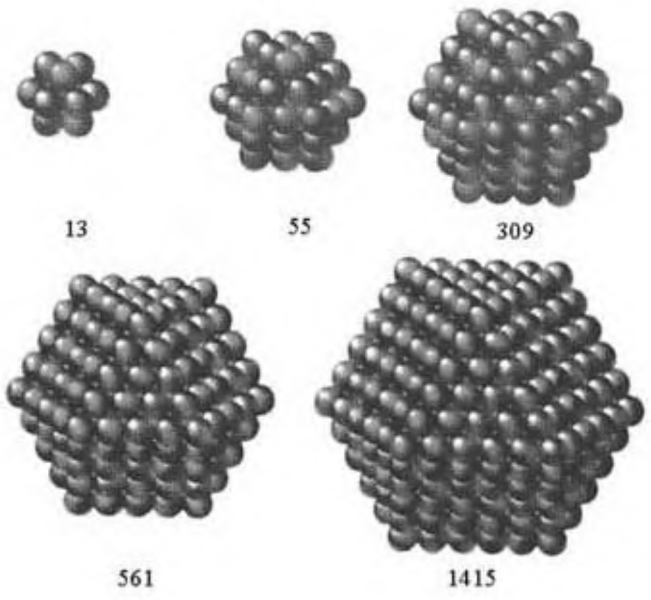

Figure 1. Metal nanocrystals with magic number of atoms in closed-shell configurations.

Electronic properties

In the nano-regime, the electronic, structural, magnetic and thermodynamic properties are essentially size-dependent[12]. A root cause for this behaviour is that the electronic energy levels in a quantum dot are not continuous as in the bulk, but are discrete, due to the confinement of the electron wavefunction in finite physical dimensions of the particle. The average electronic energy level spacing of successive quantum levels, δ known as the so-

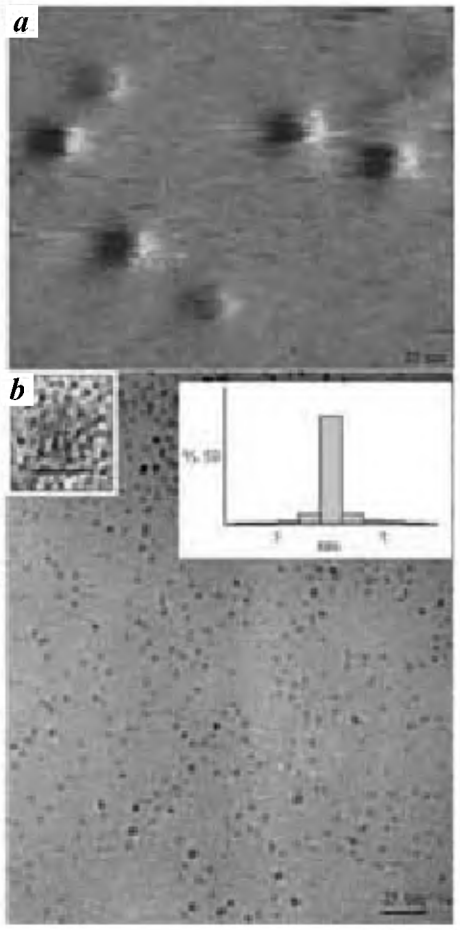

Figure 2. ***a***, STM image of polymer-coated Pd_{561} nanocrystals. The nanocrystals are seen as fluffy balls against plane background of the graphite substrate. The image was acquired with a bias voltage of 750 mV and a feedback current of 1 nA; ***b***, TEM micrograph showing isolated Pd_{561} nanocrystals. Histogram in the inset shows the distribution in the diameter. The characteristic 11[111] fringes and the icosahedral shape of an individual metal core can be seen clearly in the high-resolution micrograph shown in the inset. The diameter of the nanocrystals estimated from STM and TEM are ~ 3.4 and 2.5 nm respectively, the difference being due to the ligand shell, PVP.

called Kubo gap, is given by, $\delta = 4E_f/3n$, where E_f is the Fermi energy of the bulk material and n the total number of valence electrons in the nanocrystal. Thus, for an individual silver nanoparticle of 3 nm diameter containing approximately one thousand silver atoms, the value of δ would be 5–10 MeV (ref. 13). Tunneling measurements from this laboratory[14], have shown that clusters containing few tenths of atoms with diameters ~ 1 nm^3 are essentially non-metallic at room temperature while clusters with slightly larger diameters are metallic. It may be noted that a Pd_{561} nanocrystal with its metal-core diameter of 2.5 nm exists virtually at the metal–non metal boundary.

Work function is another property that is affected as the size is decreased. In a bulk metal, the energy required to add or remove an electron is its work function. In a molecule, the corresponding energies, electron affinity and ionization potential respectively, are however, non-equivalent. Nanocrystals being intermediary, the two energies differ only to a small extent[15], the difference being the charging energy, U. This is a Coulombic energy and is different from electronic energy gap. Further, Coulombic states can be similar for both semiconductor and metallic nanocrystals unlike the electronic states. A simple manifestation of the single electron charging is the Coulomb staircase behavior observed in the tunneling measurements[16], when a nanocrystal, covered with a suitable insulating ligand shell, is held between the probe tip and a conducting surface. The equivalent circuit is a double tunnel junction with two serial capacitors (C_1 and C_2) and two serial resistors (R_1 and R_2) arranged in parallel. According to a semi-classical model, the steps in the measured tunnel current (due to change in the electron occupancy of the nanocrystals by one) occur at voltages, $V_c = n_c e/(C + (1/C)q_0 + e/2)$, where $C = C_1 + C_2$ and q_0 is the residual charge on the nanocrystal.

For any reasonable experimental measurement of the single electron tunneling involving nanocrystals, it is important that the free ions are removed from its ligand shell. An easy way to do this is to precipitate the nanocrystals and redisperse (recrystallize) them in a fresh solvent. Thus, PVP capped Pd_{561} nanocrystals can be precipitated from aqueous solution by adding diethylether and redispersed in an ethanol–water mixture. This cycle may be repeated several times to ensure complete removal of ions from the sol. I–V measurements are performed after positioning a metallic tip over an isolated nanocrystal[17]. A Coulomb staircase obtained from atop a Pd_{561}–PVP nanocrystal is shown in Figure 3 along with the fit from the semi-classical model. The capacitance being in the aF range, Pd_{561}–PVP nanocrystals are potential candidates for single electron circuits. Such measurements have also been carried out on Pd and Au nanocrystals in the size range, 1.5–6.5 nm. It was found that the charging energies follow a scaling law of the form, $U = A + B/d$, where d is the core diameter, and A and B are constants, characteristic of the metal.

Mesoscopic organizations

It has been proposed that self-similarity in the case of metal nanocrystals would manifest in the form of a giant cluster whose shape and size are direct consequences of the nanocrystals themselves[18]. The invariance of the shell effects in metal nanocrystals with scaling is shown schematically in Figure 4. Thus, Pd_{561} nanocrystals would be expected to self-aggregate into a giant cluster of the type $(Pd_{561})_{561}$ under suitable conditions. Formation of such clusters has indeed been observed in cluster beams of Au_{55} nanocrystals. Secondary ion mass spectra obtained from the beam have indicated the presence of species

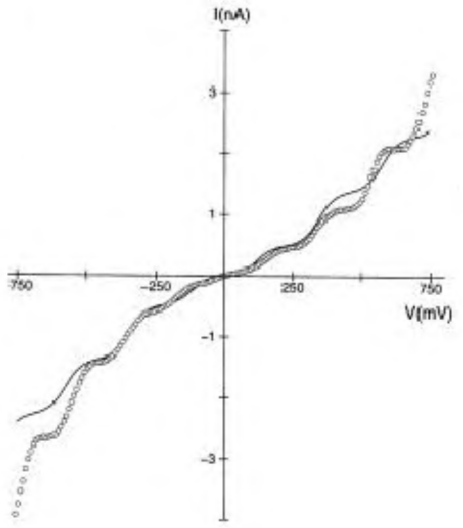

Figure 3. I–V characteristics of an isolated Pd_{561} nanocrystal (dotted line) obtained at 300 K using a STM set up. The nanocrystals were first dispersed on a highly oriented pyrolytic graphite (HOPG) substrate by drop casting. The theoretical fit (solid line) using a semiclassical model is also shown. The fit yielded capacitance: $C_1 = 0.07$ aF, $C_2 = 0.7$ aF and resistance: $R_1 = 0.5$ MΩ, $R_2 = 255$ MΩ.

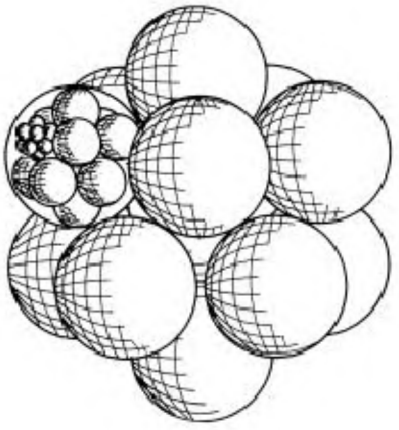

Figure 4. Self-similarity: Schematic illustration of the formation of a cluster of metal atoms (nanocrystal) and a cluster of nanocrystals (giant cluster). The size effects operating in nanocrystals could be invariant to scaling.

with large m/z values, ascribable to $(Au_{13})_{55}$ giant clusters[19]. However, studies on isolated giant clusters have proved to be difficult. In this laboratory, the monodisperse nature of the Pd_{561}–PVP nanocrystals was exploited to assist the self-aggregation process. When these nanocrystals were allowed to stand in an aqueous medium, the particles aggregated to form giant clusters[20]. The TEM micrograph in Figure 5 shows regions where the nanocrystals are densely packed in the form of aggregates (see Figure 5 *a*). Importantly, the giant aggregates exhibit discrete sizes with diameters of 9.6, 15.6, 21.6, 33.8 nm. A histogram of the observed diameters of the giant clusters is given in Figure 6. In order to calculate the number of nanocrystals in such a giant cluster, we first estimated the effective volume of a nanocrystal by measuring the shortest distance between non-aggregated particles (see Figure 2 *b*). The mean value of this distance is 4.1 nm ($\sigma < 10\%$), which matches with the diameter obtained from STM (see Figure 2 *a*). It is amazing that the estimated volume ratios show strong preference to the magic numbers. Thus, the nuclearity of the 9.6 nm giant cluster is 13 corresponding to the closure of first shell of nanocrystals. Similarly, the 15.6 nm giant cluster consists of 55 nanocrystals in two closed-shells. Giant clusters of nanocrystals with nuclearities of 147 and 561 have also been observed. The giant clusters enclosed in the respective magic diameters are depicted in Figure 5 *b*. We find excellent agreement between the experimental diameters and those calculated from the effective volume ratios. Images from the scanning electron microscope revealed the spherical shape of the giant clusters. We notice tiny spheres of ~ 10, 15 and 20 nm corresponding to the magic nuclearity giant clusters. The spherical nature of the giant clusters was also confirmed by recording TEM images at various tilt angles. The individual Pd_{561} nanocrystals involved in the formation of giant clusters exhibit the characteristic lattice image, indicating thereby that the giant clusters truly consist of an assembly of distinguishable nanocrystals.

The giant clusters could be reproducibly formed starting from Pd_{561} nanocrystals in water, ethanol and ethanol–water mixtures and from sols with a wide range of concentrations of the nanocrystals. It is possible that the formation of the giant clusters is facilitated by the polymer shell that encases them. The polymer shell seems to follow the facets of the metallic core, thereby aiding a giant assembly of the nanocrystals. The surface properties of the polymer-coated nanocrystals are clearly more favourable in that the interparticle interaction becomes sufficiently attractive. However, when covered with more directional ligands such as alkanethiols, the situation is entirely different.

In contrast to polymers, linear alkane thiols tend to self-assemble on the surfaces of nanocrystals much like in self-assembled monolayers on the corresponding metal surfaces. For example, on Au(111), the alkane thiols self-

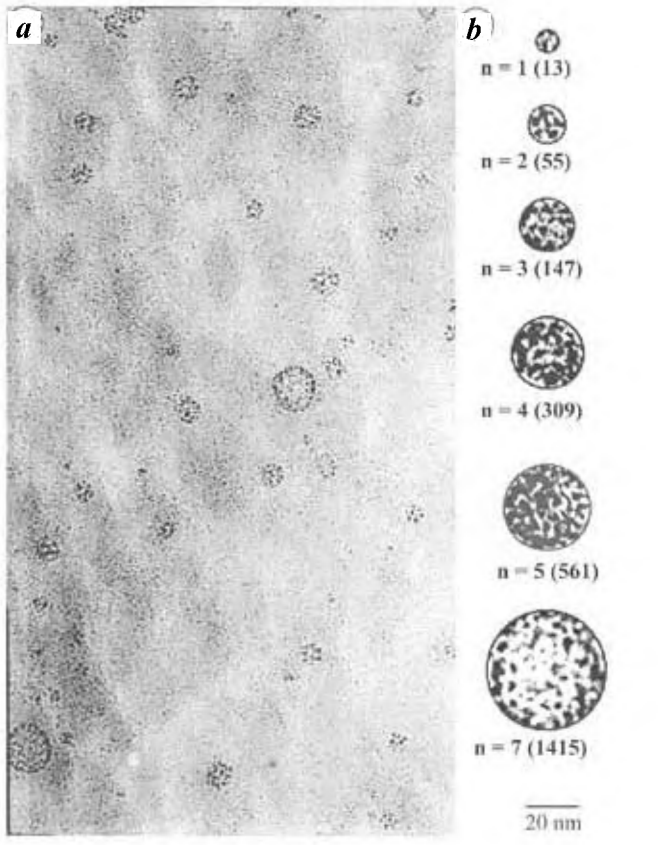

Figure 5. *a*, TEM micrograph showing the giant clusters comprising Pd_{561} nanocrystals. Sample for TEM was prepared by the slow evaporation of a PVP-Pd_{561} hydrosol; *b*, Giant clusters enclosed in circles whose diameters correspond to magic numbers. The n and (L) values indicate the number of nanocrystals and closed-shells respectively.

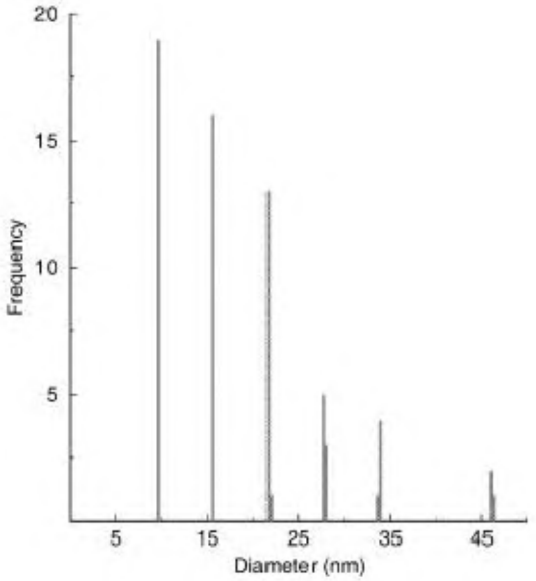

Figure 6. Histogram showing the distribution in the diameters of the observed giant clusters. The total number of giant clusters considered ~ 50.

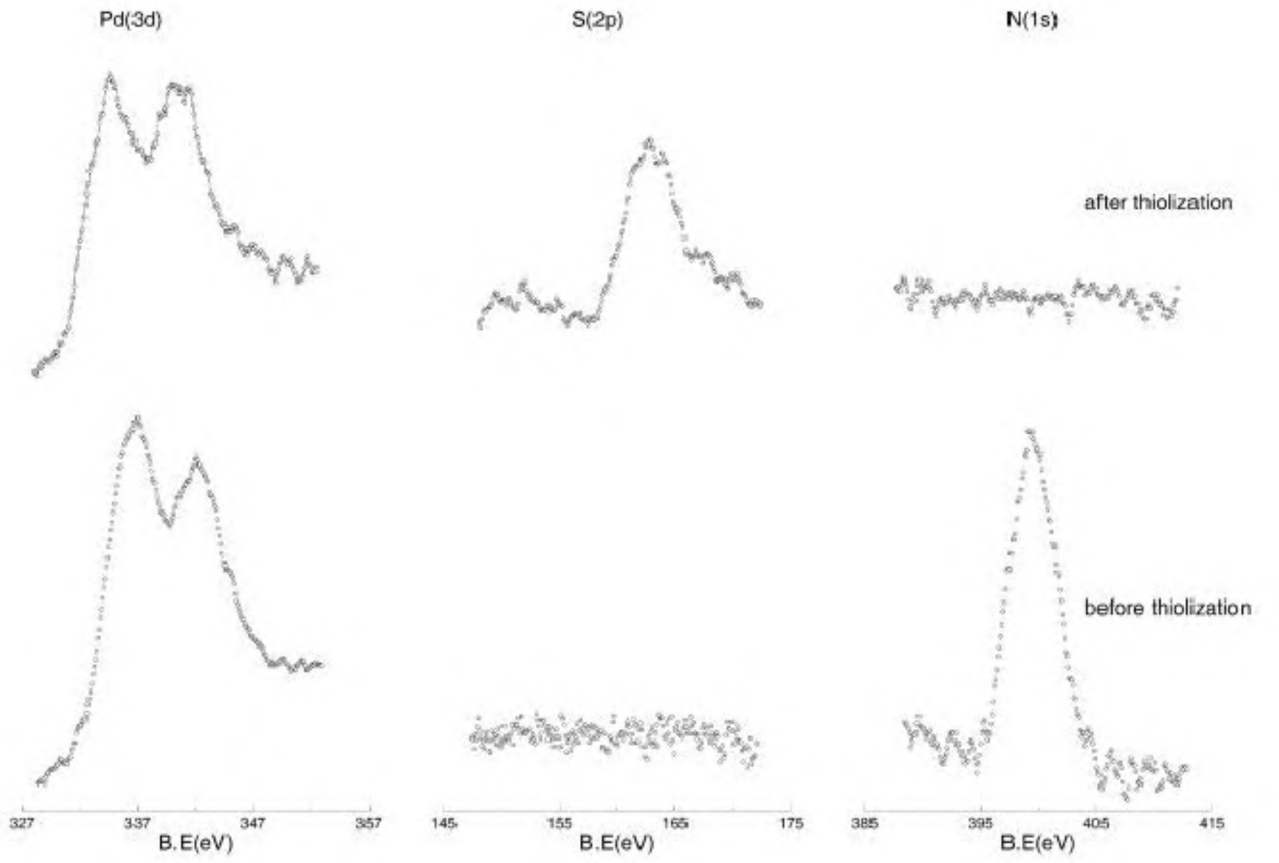

Figure 7. Core level X-ray photoelectron spectra in the Pd(3d), S(2p) and N(1s) regions for the Pd_{561} nanocrystals before and after thiolization. In both cases, the binding energy of $Pd(3d_{5/2})$ core-level is at 334 eV corresponding to metallic Pd. The N(1s) feature at ~400 eV, originating from PVP is not seen after thiolization. Instead, a new feature at 163.5 eV due to S(2p) is observed due to the chemisorbed thiol.

assemble into a dense, ordered monolayer with the alkane chains adopting a fully extended all *trans* conformation at an incline of 30° to the surface normal. The head groups arrange themselves in to $\sqrt{3} * \sqrt{3}$ R30 structure. A similar assembly on the surface of the nanocrystal, now in three dimensions with the chains extending radially outward in a brush-like arrangement, lends extraordinary stability to the nanocrystals. The thiol-capped nanocrystals can therefore withstand high temperatures and are stable for extended periods. Moreover, the thiol capped nanocrystals can also be reversibly precipitated. We have pioneered in our lab a procedure to neatly replace unwanted ligands and to redress nanocrystals with alkane thiols with no noticeable change in their size or shape[21]. The procedure can sometimes be as simple as adding few drops of concentrated HCl to a biphasic mixture of metal hydrosol and an organic solvent containing the thiol. Adopting this procedure, well-characterized nanocrystals of desired size and distribution can be transferred from aqueous sols to organic media accompanying thiol attachment. Figure 7 illustrates one such process where the PVP coating of the Pd_{561} nanocrystals is replaced by dodecanethiol molecules[22].

In addition to lending stability to nanocrystals, the alkane thiols also facilitate extended organization of nanocrystals in two dimensions. A narrow distribution in diameters and a capping agent of right dimensions is essential to bring about such an organization[22]. The organization of nanocrystals is brought about by two balancing forces – the van der Waals interaction due to polarization of the metal cores and the steric repulsion between the thiol chains that interdigitate. These two forces critically depend on the d/l factor, where d is the diameter of the nanocrystal and l the length of the thiol chain. We have found that crystalline arrays are formed for d/l values between 2 and 3. Magic nucleartiy nanocrystals are obvious candidates to study such organizations. The arrays obtained from magic nuclearity Pd_{561} and Pd_{1415} capped with dodecanethiol and octanethiol respectively is shown in Figure 8. Well-ordered two-dimensional arrays extending to a few microns are seen in either case[22]. The extent of interdigitation of the thiol chains was measured based on

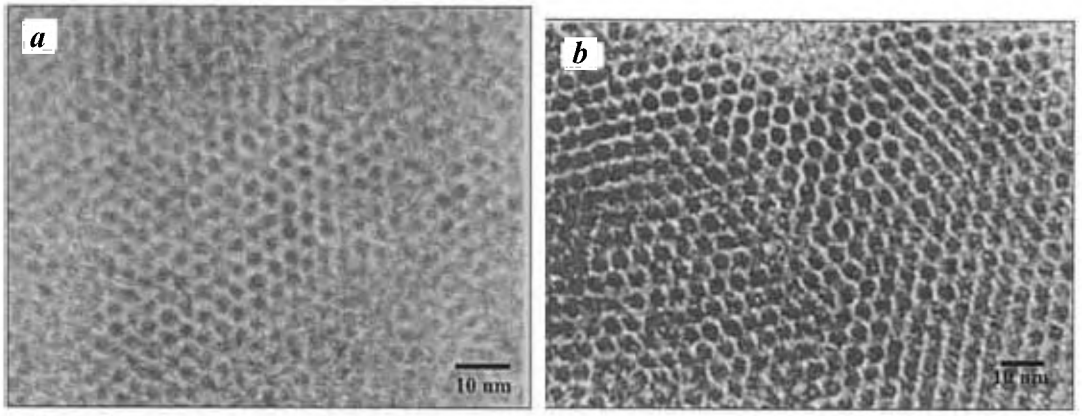

Figure 8. TEM images showing hexagonal arrays of thiolized Pd nanocrystals. ***a***, Pd_{561} octanethiol; ***b***, Pd_{1415}, octanethiol. Samples for TEM were prepared by evaporating toluene dispersions of dodecanethiol-capped Pd_{561} and Pd_{1415} nanocrystals on amorphous carbon grids.

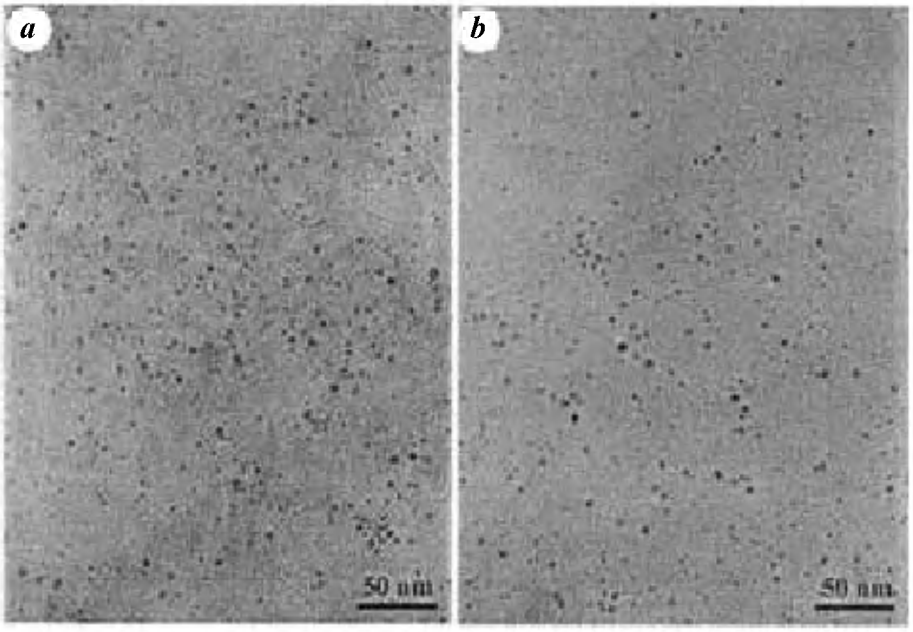

Figure 9. TEM images showing PVP capped (***a***) $Pd_{561}Ni_{8000}$ and (***b***) $Pd_{561}Ni_{10000}$ nanocrystals.

the interparticle distance and is 53% and 25% in the cases of Pd_{561}-dodecanethiol and Pd_{1415}-octanethiol.

The Pd particles can act like seeds for the reduction of Ni[23]. In our laboratory, the monosized Pd_{561} nanocrystals were exploited to synthesize Pd–Ni core-shell particles with variable Ni loading. The nanocrystals so obtained possess a core shell structure, with the Pd seed in the middle and a Ni layer covering it. Our interest was twofold to continuously vary the magnetic moment of the nanocrystals yet with a narrow size distribution and to organize the magnetic particles in two-dimensional arrays. PVP covered Pd_{561} nanocrystals were precipitated from the aqueous solution and dispersed in de-gassed propanol and refluxed under Ar atmosphere for several hours with the desired quantity of $Ni(CH_3COO)_2.4H_2O$ and PVP. Thus, $Pd_{561}Ni_n$ core-shell nanocrystals where $n = 38$, 280, 561, 800, 1500, 3000, 4500, 8000 and 10000 atoms, have been prepared. The composition of the prepared nanocrystals was analysed employing X-ray photoelectron spectroscopy (XPS) and energy dispersive analysis of X-rays (EDAX) and it was found that the composition of the obtained nanocrystals match with the feed ratios[24]. Figure 9 shows TEM images of $Pd_{561}Ni_{8000}$ and $Pd_{561}Ni_{10000}$ nanocrystals. It can readily be seen that the nanocrystals possess a uniform diameter with narrow size distribution. The mean diameters of the $Pd_{561}Ni_n$ nanocrystals, were 2.7, 2.9, 3.3, 4.9, 5.5, 6.5 and 7.0 nm for $n = 280$, 561, 1500, 3000, 4600, 8000 and 10000 respectively. Extending the synthesis by one more step, triple layer nanocrystals of the form $Pd_{561}Ni_{3000}Pd_{1500}$ (mean diameter,

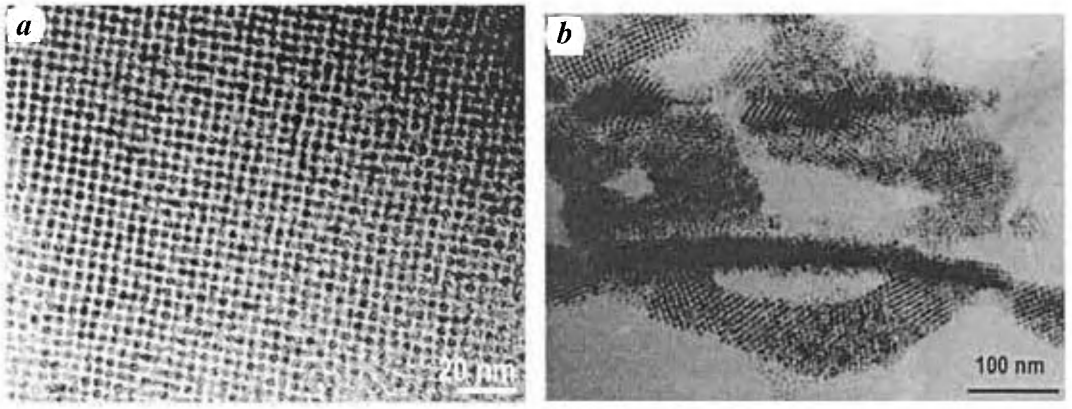

Figure 10. TEM images of an ordered array of octanethiol capped (*a*) $Pd_{561}Ni_{561}$ and (*b*) $Pd_{561}Ni_{3000}$ nanocrystals.

5.5 nm) have also been obtained. Magnetic measurements confirmed that the magnetic moment of the nanocrystals increase linearly with Ni loading. However, the superparamagnetic blocking temperature of the nanocrystals was very low, < 5 K. The $Pd_{561}Ni_n$ nanocrystals could be thiolized employing the procedure outlined above. In Figure 10, we show typical TEM images of octanethiol capped $Pd_{561}Ni_{561}$ and $Pd_{561}Ni_{3000}$ nanocrystals. It is seen that the nanocrystals organize themselves spontaneously into highly extended organizations. The projection seen in Figure 10*a* corresponds to <100> plane of a bcc lattice. In the case of higher Ni loading, the nanocrystals tend to form multilayered structures such as tapes or wires (see Figure 10*b*)[24].

Conclusions

Experimental investigations on nanocrystals, especially those with narrow size distribution, can provide in general, a deeper insight into the electronic and other properties of the quantum dots. Magic nuclearity Pd_{561} nanocrystal with a tiny metallic core (2.5 nm) is shown to work like a capacitor in the aF range by suitably covering it with an insulating polymer (PVP). It can also act as a seed for Ni, producing magnetic Pd–Ni core-shell particles with predetermined Ni loading. The Pd_{561} nanocrystals capped with PVP exhibit a tendency to self-assemble into giant clusters whose nuclearities again follow the magic number series. When coated with chain-like ligands such as long alkanethiols, the Pd_{561} as well as the $Pd_{561}Ni_n$ nanocrystals organize themselves into extended two-dimensional arrays. Such nanocrystalline assemblies may find many potential applications in nanotechnology.

1. Faraday, M., *Philos. Trans. R. Soc. London*, 1857, **147**, 145.
2. see for example: *Physics and Chemistry of Metal Cluster Compounds* (ed. de Jongh, L. J.), Kluwer, Dordrecht, 1994.
3. *Clusters and Colloids, From Theory to Applications* (ed. Schmid, G.), VCH, Weinham, 1994.
4. Rao, C. N. R., Kulkarni, G. U., Thomas, P. J. and Edwards, P. P., *Chem. Soc. Rev.*, 2000, **29**, 27.
5. Schmid, G., Bäumle, M. and Beyer, N., *Angew. Chem. Int. Ed. Engl.*, 2000, **39**, 1.
6. Martin, T. P., Bergmann, T., Göhlich, H. and Lange, T., *J. Phys. Chem.*, 1991, **95**, 6421.
7. Schmid, G., *Inorg. Synth.*, 1990, **7**, 214.
8. Vargaftik, M. N. *et al.*, *J. Chem. Soc. Chem. Commun.*, 1985, p. 937.
9. Teranishi, T. and Miyake, M., *Chem. Mater.*, 1998, **10**, 54; Teranishi, T., Hori, H. and Miyake, M., *J. Phys. Chem.*, 1997, **B101**, 5774.
10. Sun, S., Murray, C. B., Weller, D., Folks, L. and Maser, A., *Science*, 2000, **287**, 1989.
11. *Molecular Electronics* (eds Jortner, J. and Ratner, M.), Blackwell Scientific, London, 1997, IUPAC A 'Chemistry for the 21st Century' monograph.
12. Rao, C. N. R., Kulkarni, G. U., Thomas, P. J. and Edwards, P. P., *Chem. Eur. J.*, 2002, **29**, 27.
13. Edwards, P. P., Johnston, R. L. and Rao, C. N. R., In *Metal Clusters in Chemistry* (eds Braunstein, P., Oro, G. and Raithby, P. R.), Wiley-VCH, Weinham, 1999.
14. Vinod, C. P., Kulkarni, G. U. and Rao, C. N. R., *Chem. Phys. Lett.*, 1998, **289**, 329.
15. Collier, C. P., Vossmeyer, T. and Heath, J. R., *Annu. Rev. Phys. Chem.*, 1998, **49**, 371.
16. Feldheim, D. L. and Keating, C. D., *Chem. Soc. Rev.*, 1998, **27**, 1.
17. Thomas, P. J., Kulkarni, G. U. and Rao, C. N. R., *Chem. Phys. Lett.*, 2000, **321**, 163.
18. Fritsche, H. G., Muller, H. and Fehrensen, B., *Z. Phys. Chem.*, 1997, **199**, 87.
19. Feld, H., Leute, A., Rading, D., Benninghoven, A. and Schmid, G., *J. Am. Chem. Soc.*, 1990, **112**, 8166.
20. Thomas, P. J., Kulkarni, G. U. and Rao, C. N. R., *J. Phys. Chem.*, 2001, **B105**, 2515.
21. Sarathy, K. V., Raina, G., Yadav, R. T., Kulkarni, G. U. and Rao, C. N. R., *J. Phys. Chem.*, 1997, **B101**, 9876; Sarathy, K. V., Kulkarni, G. U. and Rao, C. N. R., *Chem. Commun.*, 1997, 537.
22. Thomas, P. J., Kulkarni, G. U. and Rao, C. N. R., *J. Phys. Chem.*, 2000, **B104**, 8138.
23. Teranishi, T. and Miyake, M., *Chem. Mater.*, 1999, **11**, 3414.
24. Thomas, P. J., Kulkarni, G. U. and Rao, C. N. R., *J. Nanosci. Nanotechnol.*, 2001, **1**, 267.

ACKNOWLEDGEMENT. We thank Prof. C. N. R. Rao for his constant encouragement.